99

Invited Paper

Progress in quasi-phasematched optical parametric oscillators using periodically poled $LiNbO_3$

Lawrence E. Myers
USAF Wright Laboratory, WL/AARI, Wright-Patterson AFB, OH 45433

Robert C. Eckardt, Martin M. Fejer, Robert L. Byer
E. L. Ginzton Laboratory, Stanford University, Stanford, CA 94305

Walter R. Bosenberg
Lightwave Electronics Corp., Mountain View, CA 94043

ABSTRACT

We review progress of quasi-phasematched optical parametric oscillators (OPOs) in bulk periodically poled $LiNbO_3$. We have extended the electric-field poling process so that we now reliably fabricate crystals over 60-mm long in full 3-inch-diameter, 0.5-mm-thick wafers. Periodically poled material retains the low loss and bulk power handling properties of single domain $LiNbO_3$, and QPM allows noncritical phasematching with the highest value of the nonlinear coefficient. OPOs pumped by 1.064-μm Nd:YAG lasers have been operated over the wavelength range 1.36 μm to 4.9 μm with tuning by temperature or QPM period. We have shown oscillation threshold as low as 0.006 mJ with a Q-switched pump laser, and pumping over 25 times threshold without damage. We have also demonstrated a doubly-resonant OPO pumped directly with a commercial cw diode laser at 978 nm, and a 1.064-μm-pumped cw singly-resonant OPO with threshold <3 W.

Keywords: nonlinear optics, lithium niobate, infrared sources, tunable mid-IR generation, nonlinear optical materials, frequency conversion

1. INTRODUCTION

Quasi-phasematched (QPM) optical parametric oscillators (OPOs) were introduced in the summer of 1994.[1] The enabling technology for these devices was periodically poled $LiNbO_3$ (PPLN) produced in bulk form using the technique of electric-field poling at room temperature with lithographic electrodes. This material has continued to develop with the most noteworthy improvement over the past year and a half being the increase in interaction length. The availability of long crystals of this high-gain, low-loss material has permitted rapid demonstration of a variety of QPM OPOs.

There are two important characteristics that distinguish QPM OPOs from conventional birefringently-phasematched OPOs. The first is the form of the wave-vector mismatch. Quasi-phasematching is implemented by periodically reversing the sign of the nonlinear coefficient to offset the phase velocity mismatch of the interacting waves. The mathematical expression for the wave-vector mismatch includes a grating-vector term that describes the periodic structure of the modulated nonlinear coefficient in the material. In a first-order collinear QPM device, the phasematching condition is $\Delta k_Q = \Delta k - K_g = 0$ where $\Delta k = k_p - k_s - k_i$ is the conventional wave-vector mismatch with k_p, k_s, and k_i the wave vectors of the pump, signal, and idler respectively, and $K_g = 2\pi/\Lambda$ is the grating vector of the phasematched Fourier component of the modulated nonlinear susceptibility with modulation period of Λ.[2, 3] The significance of the grating-vector term is that it can be controlled independent of other material properties so that in principle noncritical phasematching can be achieved for any interaction within the transparency range of the material.

The second difference between conventional and QPM OPOs is the nonlinear coefficient $d_Q = (2/\pi)d_{eff}$.[2, 3] First-order quasi-phasematching has lower nonlinearity by a factor of $2/\pi$ compared with an ideal phasematched process having the same nonlinear coefficient. However, because birefringence is not used to offset dispersion, the large nonlinear coefficients for parallel-polarized waves can be used. In $LiNbO_3$, this results in nonlinear drive over an order of magnitude larger than that of the most efficient birefringently phasematched process, i.e. $(2d_{33}/\pi d_{31})^2 = 20$. This, plus lack of walk-off with non-critical phasematching, makes QPM OPOs substantially more efficient than conventional devices. With the appropriate substitutions of these definitions for the nonlinear coefficient and the wave-vector mismatch, standard OPO theory applies to QPM OPOs in most respects (e.g. threshold, conversion efficiency).

0-8194-2074-3/96/$6.00

A review of QPM OPOs through early 1995 has been published.[3] In this paper, we review recent progress in QPM OPOs. In Section 2, we briefly describe the current state of the art in fabricating PPLN crystals suitable for IR devices. PPLN is having the greatest impact on low peak power devices in which the high gain is of most value in comparison with other nonlinear materials. Thus in pulsed OPOs, PPLN is particularly well suited to pumping with high-repetition-rate acousto-optically Q-switched diode-pumped solid state lasers. In addition, the broad tunability of PPLN over the spectrally important mid-IR range is of great interest. In Section 3, we describe a widely-tunable OPO pumped by an acousto-optically Q-switched diode-pumped Nd:YAG laser using a multi-grating PPLN chip which captures the most important features of QPM OPOs of this type. The ultimate in low peak-to-average power is cw pumping. In Section 4, we describe PPLN doubly resonant OPOs that are compatible with direct pumping by cw diode lasers. In Section 5, we describe the development of cw singly resonant OPOs using PPLN, which are promising as practical sources of high power coherent tunable IR radiation. PPLN OPOs will be increasingly important as the material becomes more widely available, and in Section 6, we describe prospects for future research.

2. FABRICATION OF PERIODICALLY POLED $LINBO_3$

The techniques for fabricating bulk PPLN used for the devices described in this paper have been reported elsewhere in detail.[3] A brief summary is presented here. There are two basic processing steps: preparation of an electrode structure on the surface of the substrate and electric-field poling in a high-voltage circuit. The substrate material is commercial optical-grade congruent $LiNbO_3$, typically purchased as a 0.5-mm-thick 3"-diameter wafer. The substrate is initially a single domain polarity. The surface electrode is lithographically defined with the desired pattern of the ferroelectric domains to achieve the appropriate QPM interaction. Conducting material, such as a metal film or liquid electrolyte, contacts the substrate where domain reversal is desired, and a connection is made to the poling circuit. Insulating material, such as photoresist or an oxide film, contacts the substrate where domain reversal should be prevented. The coercive field strength that must be applied for domain reversal to occur is 21 kV/mm. A liquid electrode fixture has been found to be helpful in preventing dielectric breakdown under this high field condition. The voltage is applied in one or several pulses with comparable results. After domain reversal has been accomplished and the field removed, the resulting domain structure is permanent. We have seen no change in the domain pattern in crystals prepared 2 years ago, and we have shown that domain patterns are stable even when heated to 800 °C.

This basic poling process is now routinely used to fabricate PPLN crystals with periods suitable for IR interactions. Given the dispersion of $LiNbO_3$, the required domain periods for IR devices are >10 μm. A significant advance over the past year has been the extension of the poling methods to full 3"-diameter wafers. Fabrication of full wafers of PPLN opens the door for economical commercialization of the material. It is expected that PPLN crystals and devices will soon be commercially available. The first PPLN OPOs used crystals ~5-mm long; currently crystals >60-mm long are being produced. These long crystals have been important in the experimental demonstrations that are discussed in the following sections.

3. MULTI-GRATING PPLN OPO PUMPED BY A HIGH-REPETITION-RATE ACOUSTO-OPTICALLY Q-SWITCHED DIODE-PUMPED ND:YAG LASER

The inclusion of the grating vector in the phase mismatch expression, as discussed in Section 1, is a powerful mechanism for achieving phasematching since it can be controlled by the OPO designer. Temperature and angle can also be used for tuning a QPM interaction; however, control of the grating vector means that a QPM interaction does not have to rely on inherent material properties for phasematching since the grating period is chosen to compensate the effect of material dispersion. Design of QPM devices is not limited to gratings with a single period; more sophisticated structures give specialized phasematching behavior.[2] In principle, any pattern that can be represented with a lithographic mask can be fabricated in the material. In this section, we demonstrate a QPM OPO that consists of multiple grating sections on a single PPLN chip which enables tuning across the entire mid-IR transparency range of $LiNbO_3$.[4]

3.1 Description of the multi-grating PPLN OPO experiment

Fig. 1 shows a portion of the multi-grating device. The PPLN crystals for this work were fabricated from 0.5-mm-thick congruent $LiNbO_3$ wafers. The mask design for the device consisted of grating sections that were 500-μm wide separated by 50-μm-wide insulating strips. The grating periods ranged from 26 to 32 μm in 0.25-μm increments for a total of 25 sections. This mask was used to lithographically pattern 2-μm-thick photoresist on the $+z$ surface of the $LiNbO_3$, and the resulting pattern was covered with 100-nm-thick evaporated Al. Periodic poling was performed with a field of ~21 kV/mm at a current of 20 μA for 19 sec in a liquid electrode fixture, and the diameter of the poled region was 28 mm. After poling, the PPLN pieces were annealed at 120 °C for 1 hour to relax strain at the domain walls and polished on the $\pm x$ end faces normal to the grating vectors. The crystals were not anti-reflection coated, but the ends were wedged by 0.25° to reduce etalon effects. The finished pieces used in this experiment were 26-mm long.

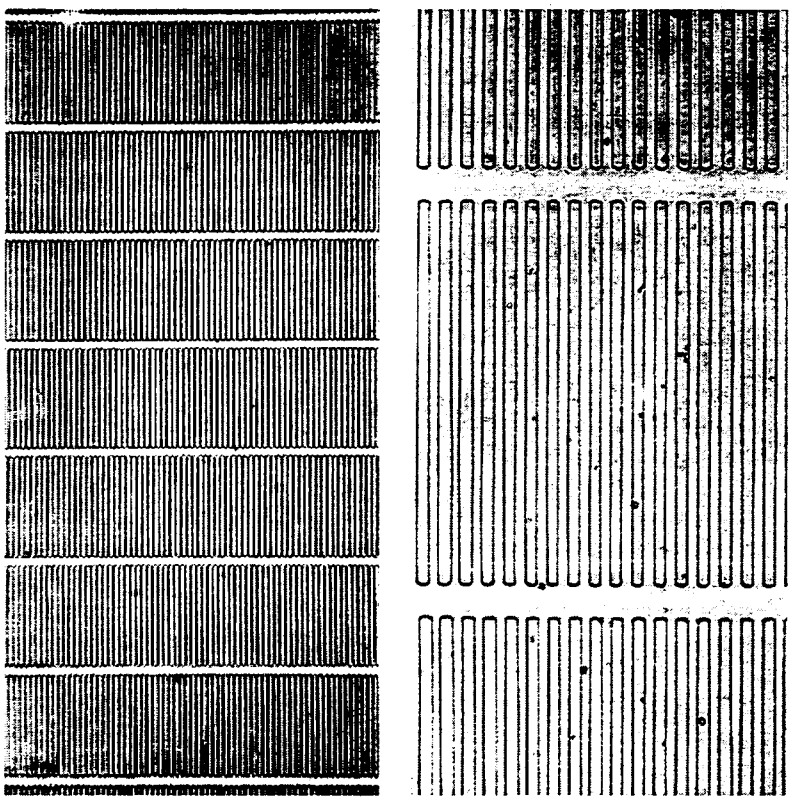

Fig. 1 Portion of the $+z$ surface of a 0.5-mm-thick PPLN chip with multiple grating regions, etched in HF acid to reveal the domain structure. The lithographic mask consists of 25 gratings with periods from 26-32 μm in 0.25-μm steps. Each grating is 500-μm wide and separated by 50-μm-wide insulating strips. The left panel shows a portion with periods 29-30.5 μm; the right panel shows a magnified view of the 29-μm period grating. The length of the finished crystals is 26 mm.

The experimental set-up is shown in Fig. 2. The pump laser was a cw-diode-pumped, acousto-optically Q-switched Nd:YAG laser operating at 1.064 μm. The laser had a pulse width of 7-20 ns when operating at 1-10-kHz Q-switch repetition rates. The laser was focused to a 47-μm spot in the crystal. The OPO cavity mirrors had 15-mm radius of curvature and were separated by 30 mm. The mirror reflectivities at the signal wavelength, centered at λ_s = 1.54 μm with a 200-nm bandwidth, were 99% and 92% for the input and output coupler respectively, with ~10% reflectivity for the pump and idler wavelengths. Losses due to Fresnel refection from the uncoated crystal surfaces were 14 %/surface for all wavelengths. The device was tuned by translating the crystal through the OPO resonator so that the pump beam interacted with different grating periods.

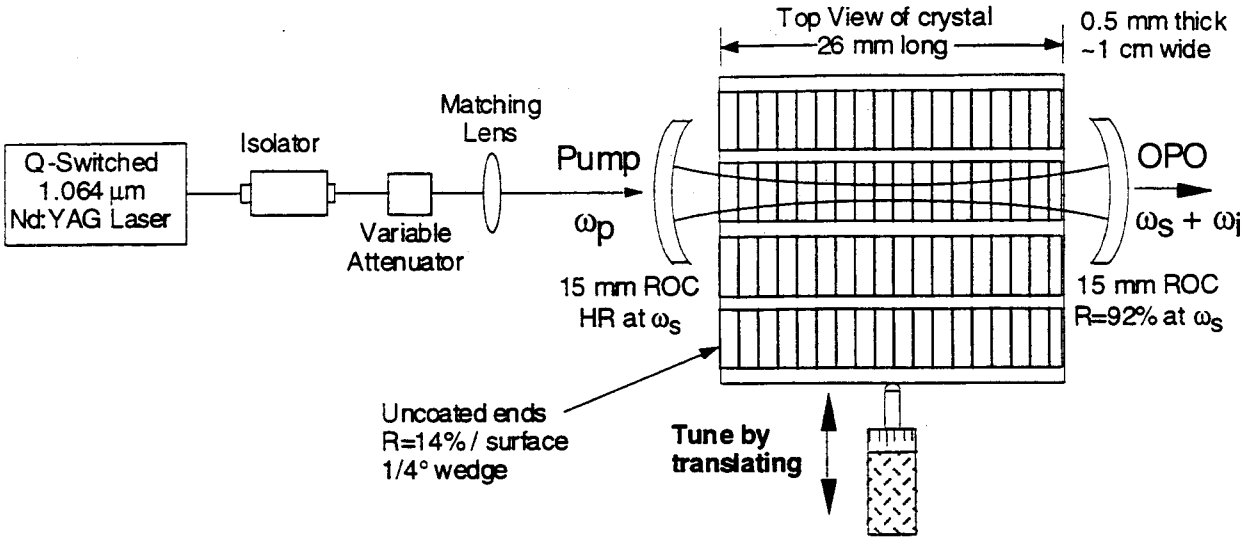

Fig. 2 Experimental set-up of the multi-grating QPM OPO. For tuning, the PPLN crystal is translated through the resonator so the pump beam interacts with different grating sections. No realignment is necessary.

Near the center of the mirror bandwidth at $\lambda_s \approx 1.54$ μm, the measured oscillation threshold was 6 μJ (0.09 J/cm^2). The OPO operated robustly even at these low pump energies; typical pump depletion was 70% at eight times threshold. The damage fluence of PPLN is the same as that for single domain $LiNbO_3$, i.e. 3 J/cm^2 for 10-ns pulses at 1.064 μm.[1, 5] We routinely achieve this value in practice. We have also observed higher damage limits when the pump energy is slowly raised due to the phenomenon of laser annealing. While the damage fluence of $LiNbO_3$ is relatively low compared to that, for example, of KTP, the high gain of PPLN allows operating well above threshold while keeping a comfortable margin below the damage limit. In our experiments, we have pumped up to 25x above threshold without damage.

3.2 Tuning of the multi-grating QPM OPO

Fig. 3 shows the tuning curve at room temperature obtained by translating the crystal through the resonator so that the pump interacts with different grating periods. The data agrees well with the phasematching calculated from the Sellmeier coefficients.[6] Note that the published Sellmeier fit is based on dispersion data for wavelengths shorter than 3.4 μm. Hence the increased deviation between our measured data and the calculation at longer idler wavelengths is expected.

The OPO ran on all grating sections from 26-μm to 31.75-μm periods. The 32-μm-period grating was not phasematched at room temperature. The OPO output tuned from 1.98-1.36 μm in the signal branch and correspondingly 2.30-4.83 μm in the idler branch. The OPO cavity mirrors required no realignment during tuning, since no tilting or beam displacement was involved. The implementation described here used 25 discrete grating sections in 0.25-μm steps. If continuous tuning is desired, a fanned grating can be fabricated, or the intermediate frequencies can be filled in with temperature fine-tuning, shown in Fig. 4, as has been previously demonstrated.[1, 7]

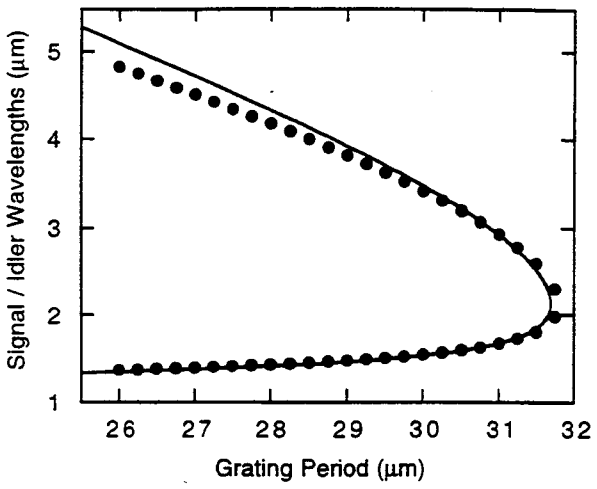

Fig. 3 Measured OPO tuning as a function of grating period. The tuning was achieved by translating the PPLN crystal ~1 cm through 24 different grating sections as shown in Fig. 2. Phasematching is noncritical for all points. Theoretical (solid) curve is calculated from dispersion.[6]

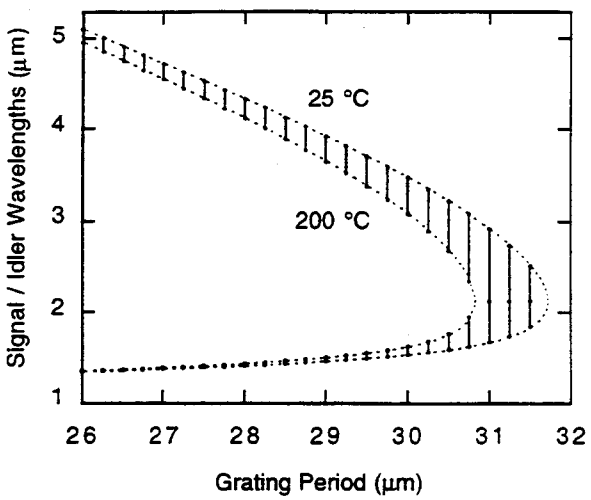

Fig. 4 Calculated tuning curve of multi-grating PPLN OPO with 0.25-μm-period steps, showing continuous tuning over wide range when translation through the grating sections is combined with temperature adjustment.

3.3 IR Operation beyond 4 μm

The idler power as a function of tuning is shown in Fig. 5. We generated up to 6 mW_{av} at 4.0 μm with 100 mW_{av} pump, and 2 mW_{av} at 4.83 μm with 150 mW_{av} pump. The modest "in-the-bucket" conversion efficiency is due to the losses of the uncoated crystal. Much of the decrease in the output power at wavelengths greater than 4 μm is due to absorption in the $LiNbO_3$. Other factors contributing to this decrease are the mirror reflectances and the reduction in idler photon energy far from degeneracy according to the Manley-Rowe relation. The performance presented here can be improved with straightforward changes; for example, anti-reflection coatings on the crystal surfaces will lower the threshold and increase conversion efficiency. Output power can be increased by increasing the pulse repetition rate as discussed in Section 3.4. We have generated up to 200 mW_{av} at 4.0 μm in a 19-mm-long PPLN crystal by pumping with 5.8 W_{av} at 10 kHz.[8]

We were initially surprised at how much power we were able to generate at wavelengths longer than 4 μm. $LiNbO_3$ is not commonly considered a useful material for generating light in this range. The IR transmission of congruent $LiNbO_3$ is shown in Fig. 6. The extraordinary polarization has a longer IR cut-off than the ordinary polarization. QPM OPOs take advantage of this using d_{33}, while the only interaction for a birefringently phasematched

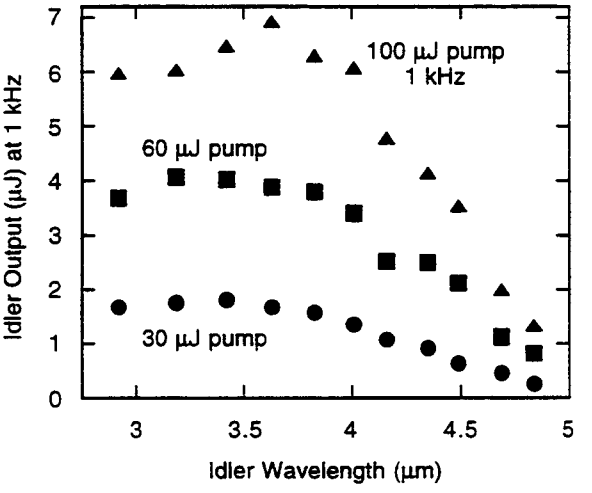

Fig. 5 Idler power for uncoated PPLN pumped with 7-ns pulses at 1 kHz. The decrease in power at longer wavelengths is due to idler absorption in the PPLN crystal, bandwidths of the cavity mirrors, and operation far from degeneracy.

OPO in $LiNbO_3$ uses Type I with ordinary polarized long-wavelength idler. The result is that QPM OPOs in PPLN have better IR performance than would be expected from past work. In addition, the extraordinary polarization is much less affected by OH absorption near 2.8 μm, so that extra processing to eliminate OH is not needed for QPM OPO crystals. In fact, the OH absorption for the extraordinary polarization may be even less than that shown in the figures because of imperfect polarizers and polarizer/crystal alignment when taking the data.

Fig. 7 shows the attenuation coefficient of $LiNbO_3$ in the IR. Note that 1-mm-long pieces have ~50% transmission for the extraordinary polarization at ~6 μm. Thus there is the possibility of output in the 5.9-6.3-μm window using the high gains available with short-pulse pump lasers. Output at 5.5 μm has been generated by single-pass difference frequency mixing in PPLN.[9]

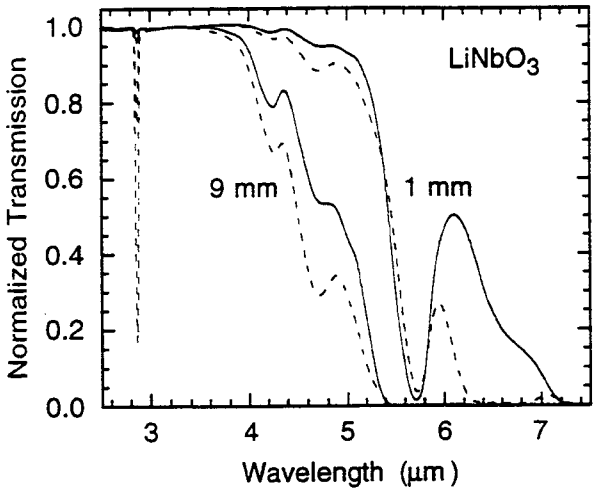

Fig. 6 Transmission of congruent $LiNbO_3$. The data have been normalized by the Fresnel reflections to give internal transmission of 1-mm and 9-mm-thick samples. Solid lines are extraordinary polarization; dashed lines are ordinary polarization. (Measurements by Richard Myers.)

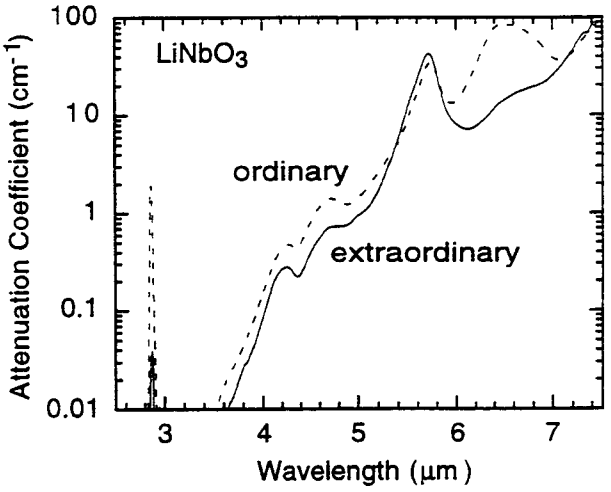

Fig. 7 Attenuation coefficient of congruent $LiNbO_3$, where power transmission = $\exp(-\alpha L)$ for crystal length L. This data is a fit to the normalized transmission of pieces 0.5-, 1-, and 9-mm long, plus a piece 25-mm long for the ordinary case.

3.4 High average power operation and photorefractive damage

Operation with high-repetition-rate lasers requires not only the capability of achieving threshold with low peak power but also handling high average power. Initially, our attempts at high-repetition-rate operation were hindered by photorefractive damage due to extraneous green light generation from non-phasematched (but enhanced) second harmonic generation of the pump. We measured photorefractive damage in an OPO using a 28.5-μm period, 9-mm-long PPLN crystal which was AR coated for the signal wavelength. The input and output couplers had 37.3-mm radius of curvature, were separated by 42 mm, and had signal reflectivities of >99% and 90% respectively. The pump laser was the same described above, focused to a 47-μm waist in the crystal. We varied the pump power by changing the repetition rate while keeping the pulse energy fixed at 0.100 mJ as shown in Fig. 3. Pumping at 0.1 W_{av} (12 kW_{av} /cm^2 at the focus), which produced 0.3 mW_{av} (70 W_{av}/cm^2) of green light, the OPO was unaffected by photorefractive damage. Pumping at 0.5 W_{av}, the OPO output decayed from its initial value on the scale of a few minutes, reaching a steady state at half of its initial value. At 1 W_{av}, the OPO quickly decayed and ceased to operate in one minute. Degradation of the OPO output was accompanied by evident fanning in the green beam, which is a typical indicator of photorefractive damage[10, 11]. The green light intensity at which photorefractive damage becomes evident is consistent with that observed by other researchers.[12]

Photorefractive damage is not permanent; it can be erased by heating the crystal so that the carriers causing the refractive index perturbation are screened or diffused. It is also well-known that photorefractive damage can be erased in real time by heating simultaneously with exposure to the damaging light,[10, 11] and we applied this in our high-repetition-rate OPO experiments. Fig. 8 shows that there is negligible degradation in the OPO output when the crystal is heated to ~100 °C for 1 W_{av} pump power (100 μJ @ 10 kHz). For the 28.5-μm period, there is essentially no change in phasematching over this temperature range, so gain parameters were constant as we varied the temperature. Around 50 °C, there is a steep improvement in the performance indicating that loss induced by photorefractive damage is eliminated.

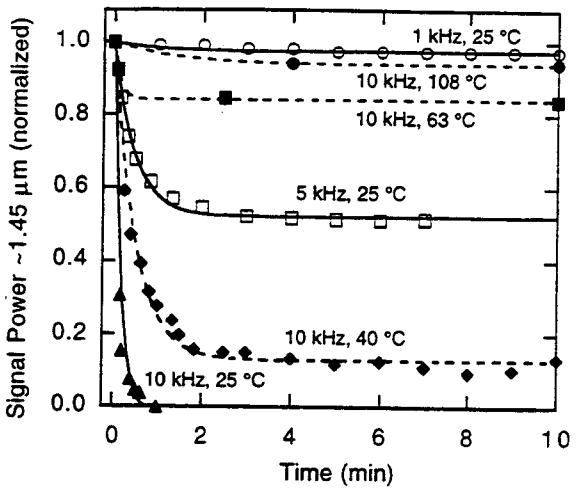

Fig. 8 OPO output power vs. time for different pumping levels with 100-μJ pulses and 46-μm waist. The PPLN crystal has 28.5-μm period. Pump pulse length was 7 ns at 1 kHz and 19 ns at 10 kHz.

The importance of this experiment is that photorefractive damage can be controlled with operation at temperatures ~100 °C allowing the average power of the pump source to be increased. Design of crystals for operation at elevated temperature is no different than for operation at room temperature. The correct grating period is calculated using the temperature-dependent refractive indices and the thermal expansion of the material at the desired operating point. High-power operation has been demonstrated with a high-repetition-rate cw-diode-pumped Q-switched 1.064-μm Nd:YAG laser (Lightwave Electronics Model 210S) using a 15-mm-long 29.5-μm-period PPLN crystal with 5.8-W pump power over the range 10-20 kHz. 2 W at 1.54 μm and 0.6 W at 3.45 μm were generated at 70 °C.[8]

3.5 Summary of multi-grating PPLN OPO

The multi-grating OPO demonstrates many of the important features of QPM OPOs based on PPLN. The flexibility of engineering the phasematching through design of the lithographic mask used in poling is illustrated in this device by the fabrication of multiple grating sections on a single chip. This design permits wide tunability with noncritical phasematching across the entire mid-IR transparency range of $LiNbO_3$. The demonstrated tuning range out to 4.83 μm is a consequence of better long-wavelength transmission which is available to QPM OPO implementations. Low threshold (6 μJ) and high conversion efficiency (>70%) are achieved with the d_{33} nonlinear coefficient accessible through quasi-phasematching. Scaling to high average power by increasing the repetition rate of the pump laser is practical since PPLN can operate well with the lower peak energy of these pulses. Photorefractive damage at higher pump power can be eliminated by heating and quasi-phasematching can be adjusted for any specified operating temperature. These features make QPM OPOs promising candidates for applications with acousto-optically Q-switched cw-diode-pumped solid-state pump lasers which are now undergoing rapid commercial development.

4. DOUBLY-RESONANT OPOS WITH DIRECT DIODE PUMPING

We previously reported on a cw doubly-resonant OPO (DRO) that was directly pumped by a commercial cw diode laser. The high gain of PPLN was important in lowering the threshold of this device, and quasi-phasematching was essential in matching the crystal to the wavelengths of readily available diode lasers. With a 9-mm-long PPLN crystal, we obtained thresholds as low as 61 mW when pumped by a 980-nm diode MOPA laser. With the longer crystals now available , we can easily expert thresholds compatible with pumping by single stripe diode lasers.

The disadvantage of DROs is the frequency and amplitude instability arising from the requirement of simultaneously satisfying two resonance conditions. Thus even small perturbations in cavity length, temperature, or pump frequency cause

mode hops. Monolithic resonator designs have been used to improve the stability of DROs. Towards that end, we fabricated a monolithic DRO ring resonator using PPLN.[13] The experimental layout is shown in Fig. 9. We have operated this device using a Nd:YAG nonplanar ring oscillator as the pump laser and have achieved thresholds comparable to those of our original diode-pumped DRO. Future efforts will investigate single-frequency stabilization, electro-optic tuning, and pumping with external cavity tunable diode lasers.

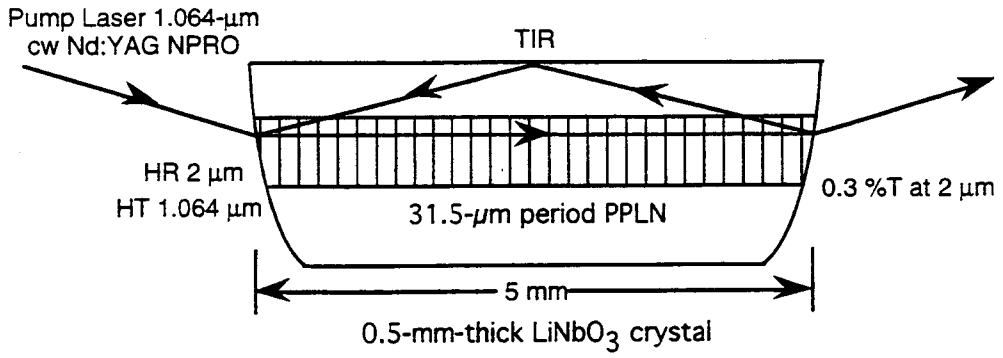

Fig. 9 Monolithic ring resonator fabricated in $LiNbO_3$ with a PPLN section. This OPO was designed for an experiment involving frequency locking to Xe* at 2.19 μm. The PPLN period of 31.5 μm phasematched at 52 °C with a 1.064-μm pump. The polished ends are spherical with 4-mm radius of curvature and dielectric mirror coatings. The side is polished flat with no coating for a TIR bounce.

5. CW SINGLY-RESONANT OPOS IN PPLN

The instabilities of the DRO make singly-resonant OPOs (SROs) desirable; however, the high thresholds of cw SROs have made these devices nearly unattainable. The first cw SRO was demonstrated by Yang.[14] This was a 0.532-μm-pumped KTP device with a threshold of 1.4 W using a double-passed pump. Later a ring-cavity SRO was built which had a threshold of 4.3 W with a single-pass pump and produced 1.9 W at $\lambda_i = 1.039$ μm.[15] No significant tuning was possible because of the insensitivity of the dispersion to temperature changes and because of the high gain requirement which forbid any operation off the peak of phasematching. Despite the limited utility of this device, it demonstrated the important result that SRO behavior was possible when pumping several times above threshold even with some amount (~1%) of round-trip idler feedback.[16]

The high gain and low loss of PPLN have recently enabled us to demonstrate practical cw SROs with stable, efficient, single-frequency output using simple cavities and commercially-available pump laser powers.[17, 18] Low threshold and adjustable quasi-phasematching of a PPLN SRO permit direct pumping with 1.064 μm for a useful source of coherent cw radiation tunable over the spectrally important mid-IR range from 1.3 μm to ~5 μm.

The crystals for this cw SRO were 50-mm long with 29.75-μm period, which quasi-phasematched at 1.57-μm signal and 3.45-μm idler with 1.064-μm pumping at 175 °C. The same fabrication recipe, employed previously on smaller pieces of $LiNbO_3$, worked successfully on the full 3-inch-diameter, 0.5-mm-thick wafers used here.

The experimental set-up is shown in Fig. 10. The pump laser is diode-pumped Nd:YAG producing 17 W cw of polarized multi-longitudinal-mode output at 1.064 μm. 13 W is available to pump the OPO. The pump beam is focused to a 97-μm waist radius in the crystal. The OPO resonator is a simple two-mirror symmetric linear cavity with round-trip signal loss of ~2% and round-trip idler loss of >99%.

Fig. 11 shows the OPO output vs. pump input. The threshold of 4.5 W agrees reasonably well with a calculated value of 3.7 W for a single-frequency pump laser,[19] indicating that all the laser modes pump a single mode of the resonant wave in an SRO.[20] The focusing parameter for this measurement is $\xi = L/b = 0.42$ where L is the crystal length and b is the confocal parameter of the pump (or signal) in the crystal. By focusing more tightly to give $\xi = 0.62$, 1.0, and 1.6, we lowered the

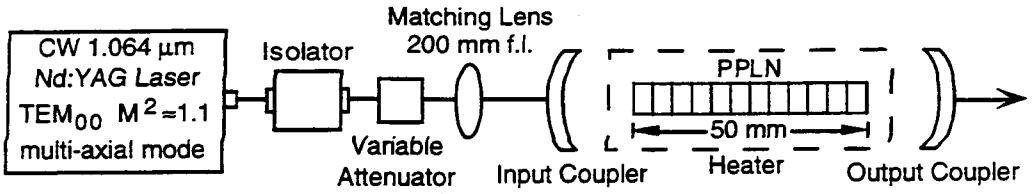

Fig. 10 Experimental set up of cw SRO in PPLN. Mirrors have 50-mm radii of curvature and are separated by 104 mm. Reflectivities of the pump, signal, and idler are 2%, 99.7%, 3% for the input coupler, 14%, 99.5%, 11% for the output coupler, and 6%, 0.3%, 7% for each surface of the PPLN crystal.

oscillation threshold to 4.2 W, 2.9 W, and 2.6 W respectively. However, tighter focusing caused a sudden increase in amplitude noise of the OPO output when the pump power was raised above 1.7x threshold. This sudden increase in noise was very repeatable. It is not yet clear if this behavior is intrinsic to a cw SRO with tight focusing or an experimental effect (e.g. thermal). With loose focusing, low noise operation was obtained even pumping 3x above threshold.

The spectral qualities of the OPO signal output were observed using solid etalons. Despite a pump laser linewidth of ~2.2 GHz FWHM corresponding to ~9 longitudinal modes, the resonated signal wave operated on a single longitudinal mode with linewidth <0.02 cm^{-1} (0.5 GHz). As shown in Fig. 12, the free-running OPO stayed on one longitudinal mode for 10-20 sec until drift of cavity length or temperature caused a mode hop. When the cavity length was scanned, the OPO stayed on a single cavity mode over >75% of the free spectral range, indicating the singly-resonant nature. For a comparable DRO, mode hops occur for 2-nm cavity length change or 3-MHz pump frequency shift, over two orders of magnitude more stringent than the tolerances of the SRO.

While this device can be temperature tuned, operation <110 °C is limited by photorefractive damage as shown in Fig. 13. Tuning by changing the quasi-phasematching period provides wide tunability at fixed temperature. Using a 25-mm long PPLN crystal with multiple grating sections like that described in Section 3.1, we tuned the output from 1.62-1.46 μm (signal) and 3.11-3.95 μm (idler), limited by losses of the optical coatings. With the right optics, this cw SRO can tune across the entire mid-IR transparency range of $LiNbO_3$ 1.3 μm to >4 μm.

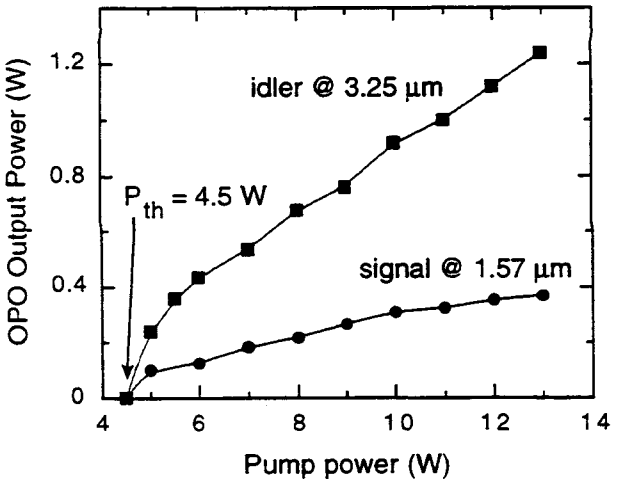

Fig. 11 OPO output vs. pump input power for 29.75 μm period PPLN at 175 °C. The maximum output is 1.25 W at 3.25 μm pumping with 13 W at 3x above threshold. Signal power is low because of the low output coupling used. With tighter focusing, thresholds <2.6 W were obtained.

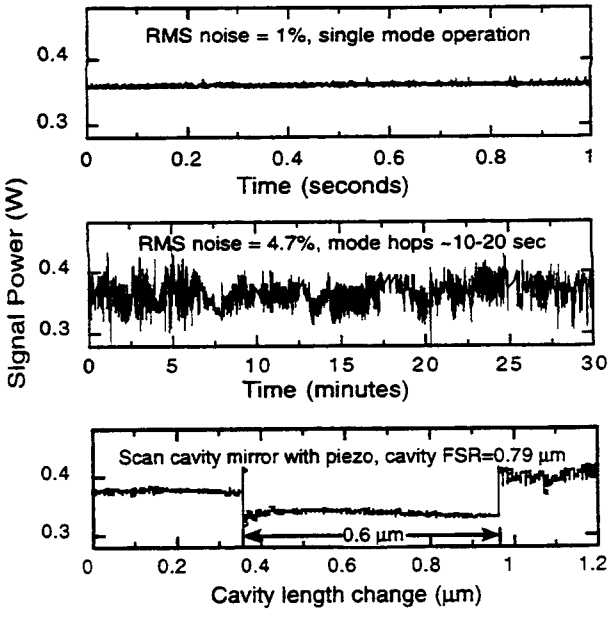

Fig. 12 Stability of OPO signal power in PPLN cw SRO, with 6.7 W pump (2x threshold).

We also operated the PPLN cw SRO using a four-mirror ring cavity in a bow-tie configuration. The threshold of this OPO was higher because of the additional optics, but it could be tightly focused without the increased noise seen in the linear cavity. The conversion efficiency was also much higher as shown in Fig. 14. Using the multi-grating piece described above, we obtained >1 W idler power over the tuning range 3-3.8 μm, and 0.6 W at 4 μm. The above-threshold behavior of cw SROs will be investigated in future experiments and theoretical modeling.

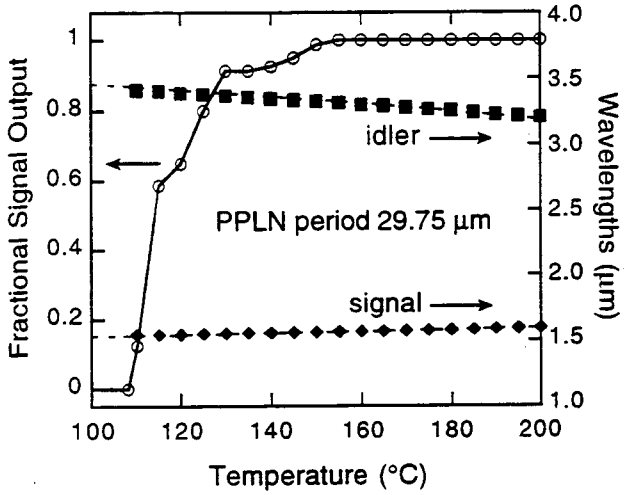

Fig. 13 Heating the crystal eliminates photorefractive damage during OPO operation. Temperature tuning is possible as shown, but adjusting the quasi-phasematching period with a multi-grating PPLN chip gave broader tuning over 1.62-1.46 μm (signal) and 3.11-3.95 μm (idler) at 175 °C for PPLN periods 30-28 μm.

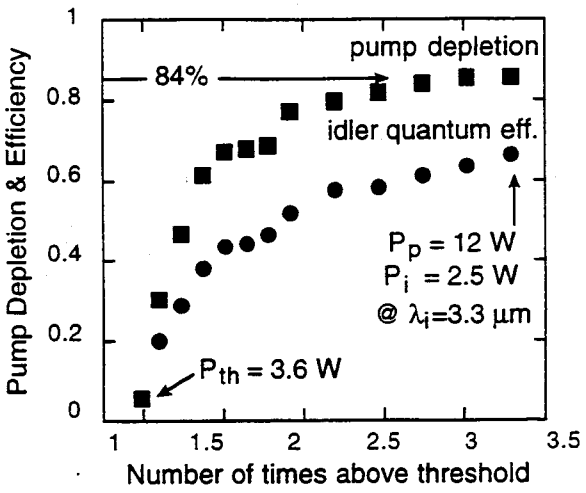

Fig. 14 Pump depletion and idler quantum efficiency in the 4-mirror ring-cavity cw SRO. Pump depletion was 84% at 3x above threshold. Extracting this converted pump as idler was 76% efficient due to losses in the optical coatings. Idler power was 2.5 W with 12 W of pump for optical power conversion efficiency of 21%.

6. CONCLUSION

QPM OPOs based on bulk PPLN have shown exceptional progress over the past year and a half since their introduction. The multi-grating device highlights many of the desirable features of a QPM OPO. It has low threshold, efficient pump conversion, and noncritical phasematching tunable across the entire mid-IR transparency range of $LiNbO_3$ from 1.3-5 μm. The ability to fabricate sophisticated grating designs such as this illustrates the control of ferroelectric domain patterning now possible in electric-field-poled bulk PPLN. These capabilities have led to >5-cm-long crystals fabricated from full wafers, which permitted the demonstration of a practical cw SRO. This device promises to be important as a source of stable, coherent, high-power, mid-IR radiation.

The fabrication capability of PPLN is continuing to advance. Fabrication of shorter gratings periods, needed for visible light generation, is the subject of much current research. Thick substrates are important to allow a larger working aperture for practical, low-loss resonators and for scaling the peak-power handling capability. We have recently demonstrated progress towards poling of 1-mm thick wafers.[21] In the future, the ability to control phasematching through domain patterning will lead to combined nonlinear processes in a single device, such as difference-frequency or sum-frequency generation from OPO outputs.

ACKNOWLEDGMENTS

We thank Crystal Technology, Inc. for supplying $LiNbO_3$ wafers. This work was supported by US Air Force Wright Laboratory, Wright-Patterson AFB, OH, and ARPA through the Center for Nonlinear Optical Materials at Stanford University.

REFERENCES

1. L. E. Myers, G. D. Miller, R. C. Eckardt, M. M. Fejer, R. L. Byer, and W. R. Bosenberg, "Quasi-phasematched 1.064-μm-pumped optical parametric oscillator in bulk periodically poled $LiNbO_3$," Opt. Lett. **20**, 52-54 (1995).
2. M. M. Fejer, G. A. Magel, D. H. Jundt, and R. L. Byer, "Quasi-phase-matched second harmonic generation: tuning and tolerances," IEEE J. Quantum Electron. **28**, 2631-2654 (1992).
3. L. E. Myers, R. C. Eckardt, M. M. Fejer, R. L. Byer, W. R. Bosenberg, and J. W. Pierce, "Quasi-phasematched optical parametric oscillators in bulk periodically poled $LiNbO_3$," J. Opt. Soc. Am. B **12**, 2102-2116 (1995).
4. L. E. Myers, R. C. Eckardt, M. M. Fejer, R. L. Byer, and W. R. Bosenberg, "Multi-grating quasi-phasematched optical parametric oscillator in periodically poled $LiNbO_3$," accepted for publication in Opt. Lett. (1996).
5. S. J. Brosnan and R. L. Byer, "Optical parametric oscillator threshold and linewidth studies," IEEE J. Quantum Electron. **15**, 415-431 (1979).
6. G. J. Edwards and M. Lawrence, "A temperature-dependent dispersion equation for congruently grown lithium niobate," Opt. Quantum Electron. **16**, 373-374 (1984).
7. V. Pruneri, J. Webjörn, P. St. J. Russell, and D. C. Hanna, "532 nm pumped optical parametric oscillator in bulk periodically poled lithium niobate," Appl. Phys. Lett. **67**, 2126-2128 (1995).
8. W. R. Bosenberg, A. Drobshoff, and L. E. Myers, "High-power, high-repetition-rate optical parametric oscillators based on periodically poled $LiNbO_3$," in *Advanced Solid State Lasers*, 1996 Technical Digest Series, (Optical Society of America, Washington, DC, 1996), p. 68-70.
9. L. Goldberg, W. K. Burns, and R. W. McElhanon, "Widely tunable difference frequency generation in QPM-$LiNbO_3$," in *Conference on Lasers and Electro-Optics*, Vol. 15, 1995 OSA Technical Digest Series, (Optical Society of America, Washington, D.C., 1995), paper CPD49.
10. A. Ashkin, G. D. Boyd, J. M. Dziedzic, R. G. Smith, A. A. Ballman, J. J. Levenstein, and K. Nassau, "Optically-induced refractive index inhomogeneities in $LiNbO_3$ and $LiTaO_3$," Appl. Phys. Lett. **9**, 72-74 (1966).
11. M. Taya, L. E. Myers, G. D. Miller, M. M. Fejer, and R. L. Byer, "High resistance to photorefractive damage in periodically poled bulk $LiNbO_3$," in *CNOM Annual Report*, (Center for Nonlinear Optical Materials, Stanford University, Stanford, CA 94305, 1994), p. 60-61.
12. Y. Furukawa, M. C. Bashaw, and M. M. Fejer, "Investigation of beam degradation in $LiNbO_3$," in *CNOM Annual Report*, (Center for Nonlinear Optical Materials, Stanford University, Stanford, CA 94305, 1993), p. 38-40.
13. This experiment was conducted in collaboration with Rob Batchko, Uwe Sterr, and Konstantin Fiedler.
14. S. T. Yang, R. C. Eckardt, and R. L. Byer, "Continuous-wave singly resonant optical parametric oscillator pumped by a single-frequency resonantly doubled Nd:YAG laser," Opt. Lett. **18**, 971-973 (1993).
15. S. T. Yang, R. C. Eckardt, and R. L. Byer, "1.9-W cw ring-cavity KTP singly resonant optical parametric oscillator," Opt. Lett. **19**, 475-477 (1994).
16. S. T. Yang, R. C. Eckardt, and R. L. Byer, "Power and spectral characteristics of continuous-wave parametric oscillators: the doubly to singly resonant transition," J. Opt. Soc. Am. B **10**, 1684-1695 (1993).
17. L. E. Myers, W. R. Bosenberg, W. M. Tulloch, M. A. Arbore, R. C. Eckardt, M. M. Fejer, and R. L. Byer, "CW singly-resonant optical parametric oscillators based on 1.064-μm-pumped periodically poled $LiNbO_3$," in *Advanced Solid State Lasers*, (Optical Society of America, Washington, D.C., 1996).
18. W. R. Bosenberg, A. Drobshoff, J. I. Alexander, L. E. Myers, and R. L. Byer, "Continuous-wave singly-resonant optical parametric oscillator based on periodically-poled $LiNbO_3$," submitted to Optics Letters (1996).
19. S. Guha, F.-J. Wu, and J. Falk, "The effects of focusing on parametric oscillation," IEEE J. Quantum Electron. **18**, 907-912 (1982).
20. S. E. Harris, "Tunable optical parametric oscillators," Proc. IEEE **57**, 2096-2113 (1969).
21. L. E. Myers, T. P. Grayson, W. R. Bosenberg, M. D. Nelson, V. Dominic, M. M. Fejer, and R. L. Byer, "Increasing the aperture of electric-field periodically-poled $LiNbO_3$," submitted to CLEO 1996.